

Deployment of a High Sensor-Count SHM of a Prestressed Concrete Bridge Using Fibre Optic Sensors



F. I. H. Sakiyama, F. Lehmann, and H. Garrecht

Abstract To deploy an accurate safety-relevant structural health monitoring, one must assure the utmost care and in-depth knowledge of the monitored structure, which may present challenges such as the reliability to detect unexpected anomalies due to the failure of a component, the correct setting of thresholds and triggers to discern changes due to environmental conditions from critical events, and the high expense in terms of hardware and personnel availability. The fibre optic (FO) technology can provide integrated sensing along with extensive measurements lengths with high sensitivity, durability, and stability, which makes them ideal for SHM of concrete structures. Therefore, an SHM system using quasi-distributed FO FBG sensors is proposed to continuously monitor the strain changes of a 57 m long prestressed concrete bridge due to traffic loads and environmental changes. A total of 89 long-gauge strain sensors were installed to monitor the strain distribution in two lines along the complete length and five arrays in the shear direction. Additionally, 2 FO acceleration sensors and 94 FO FBG temperature sensors were installed for correct and precise temperature compensation of the strain sensors and to correctly detect the strain changes due to temperature variation on the bridge. In this work, the installation processes of the FO sensors and the operational hardware is shown. Furthermore, initial measurement values are presented to demonstrate the potential of FO to provide a reliable SHM system to monitor large concrete structures.

Keywords Structural health monitoring · Fibre optic sensors · Fibre bragg gratings · Prestressed concrete maintenance

F. I. H. Sakiyama (✉) · F. Lehmann · H. Garrecht
Materials Testing Institute, University of Stuttgart, Stuttgart, Germany
e-mail: felipe.sakiyama@ufvjm.edu.br

F. I. H. Sakiyama
Federal University of the Jeq. and Muc. Valleys, Teófilo Otoni, Brazil

1 Introduction

1.1 Overview

The early detection of cracks in concrete structures is a common practice within building inspection procedures, as it can be a good indicator for necessary maintenance or reinforcement measures of damaged structures. Likewise, documenting any progress of existing cracks is essential to differentiate between static and dynamic damage states, and thus to enable the assessment of the cracks relevance concerning durability and stability; therefore, existing and new cracks and their lengths are recorded during periodic building inspections.

The interval of such on-site inspections is usually every six years, but it can vary between different standards and according to the current structure condition. Although this has worked well in the past, every year the traffic load increases on old bridges that have been reaching its lifespan or which are known not to meet today's demands both on the load capacity and in terms of the construction method and the materials used [1].

Under these circumstances, significant damage can go unnoticed between inspections, with an increasing probability every year. Also, the periodic inspection depicts the state of the building only at the time of inspection and is influenced by the inspector's subjectivity [9]; hence, particularly high loads in the period between, e.g. from heavy traffic events or temperature, are not taken into account unless this has already caused visible damage. Periodic inspections alone are insufficient for maintaining the health of structures and assuring the users' safety [2].

Structural health monitoring (SHM) offers a way to supplement regular building inspections [10]. For this purpose, sensors are installed at suitable locations on the building, which continuously record, save and transmit information about the structure's behaviour. Ideally, this data is automatically evaluated, and an alarm is triggered when specified limit values are exceeded. However, this often proves to be difficult in practice, since the real structural behaviour, particularly in the case of load redistribution and crack formation, deviates from the underlying idealised model, and therefore cannot be evaluated solely by software. Thus, limit values are often set based on the usual fluctuation range of the measured parameters based on the previous continuous monitoring, and the measurement data is interpreted manually.

The selection of suitable sensors takes place in the balance between spatial resolution, number of sensors and sensitivity. For example, the natural frequencies of a building can be determined with just a few vibration velocity sensors, and global changes in load behaviour can be inferred from this; however, damage to the structure must already be considerable. In contrast, strain gauges, e.g., offer the possibility of detecting the smallest changes in crack widths or local strains; however, an extraordinarily large number of sensors would be necessary to be able to monitor the entire structure.

Although the current approaches of SHM systems using traditional single-point sensors—such as electric strain sensors, accelerometers, and GPS-based

sensors—have appropriate measurement precision for SHM purposes [8], they present challenges when deployed in real scale applications [6], given the limited number of possible points to assess the structural behaviour and the harsh environmental conditions during operation [4]. When it comes to reinforced concrete structures, the development of health monitoring and damage identification presents further challenges, since this type of structure is affected by a variety of chemical, physical and mechanical degradation processes, and has a heterogeneous composition and nonlinear behaviour [8]. On the other hand, the fibre optic (FO) technology can provide integrated sensing along with extensive measurements lengths with high sensitivity, durability, and stability, which makes them ideal for SHM of concrete structures [7].

The Fibre Bragg Grates (FBG) based FO sensors, for instance, offer new approaches, in particular for the detection of new cracks, since it enables high-resolution ($\sim 1 \mu\text{m}$) strain monitoring over discrete segments. Within these segments, crack openings, e.g., can be detected without the previous knowledge of their locations.

Many researches have already been done on the topic of crack detection in concrete, but the application on real structures is still missing. This project aims to investigate the possibilities and limits of fibre-optic building monitoring, especially concerning the detection of cracks. Therefore, an SHM system using quasi-distributed FO FBG sensors is proposed to continuously monitor the strain changes of a 57 m long prestressed concrete bridge due to traffic loads and environmental changes. In this work, the installation processes of the FO sensors and the operational hardware is shown. Furthermore, initial measurement values are presented to demonstrate the potential of FO to provide a reliable SHM system to monitor large concrete structures.

1.2 *FBG Sensing Technology*

An FBG sensor is a microstructure with 5 to 10 mm in length [11] and consists of a series of evenly spaced etchings at a tuneable distance Λ from each other, written using a UV laser in the core of a standard telecom FO [5]. When the light passes through the FO, a portion of the light is reflected at each etching, where the spacing of the etchings causes the reflected light to have a different phase for most wavelengths; thus, destructive interference causes the individual reflections to cancel each other out. However, the wavelength harmonic to the etching spacing will be reflected in phase and experience constructive interference. Hence, the reflected spectrum λ_B (or Bragg wavelength) will contain essentially one wavelength, which can be directly related to the etching spacing [3], as illustrated in Fig. 1. If the FO is subjected to external loads, e.g., strain or temperature variation, the fibre's length and consequently the spacing between the gratings will change, causing a shift in the Bragg wavelength. With the proper calibration, the external load can be quantified from the Bragg wavelength shift.

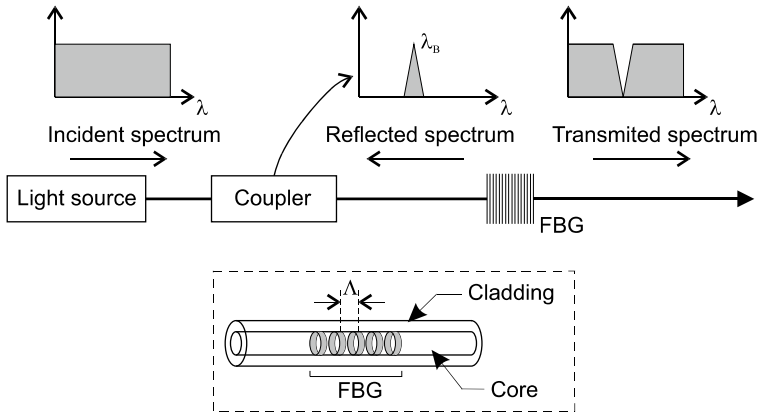


Fig. 1 Measurement principle of the FBG sensor [13]

The long-gauge FBG sensors (LGFBG), also known as quasi-distributed FO sensors, are characterised by their in-lie multiplexing feature, whereby a series of individual sensors can be connected and measured in a single fibre-array using techniques such as wavelength-division multiplexing (WDM). When combined with the long-gauge attribute, the integral length of a structure can be monitored with a distributed, yet discrete, array of sensors; thus the name “quasi-distributed”. The discretisation resolution, i.e. the smallest distance wherein changes can be measured, is determined by the gauge’s length of the sensors, ranging from millimetres up to 10 m long [12].

More details about FBG sensors and their application can be found in [10].

2 SHM System

2.1 Monitored Structure Characterisation

The monitored structure is a prestressed hollow-core concrete bridge built in 1964. The design load class is 60/30, according to DIN 1072. With a width of 11.08 m, it has three continuously spans with a total length of 57.00 m (17.00–23.00–17.00 m) without coupling joints (Figs. 2 and 3). The two centre columns are designed as individual supports with pot bearing. On the southern abutment, the superstructure is supported by two linear rocker bearings, and on the northern abutment, by two roller bearings.

Like most of the prestressed concrete structures designed until the ’70s in Germany, the bridge was built with prestressing steel types St 145/60 Sigma, KA 141/40 and KA35/10, which are known for their high vulnerability to corrosion-induced cracking.

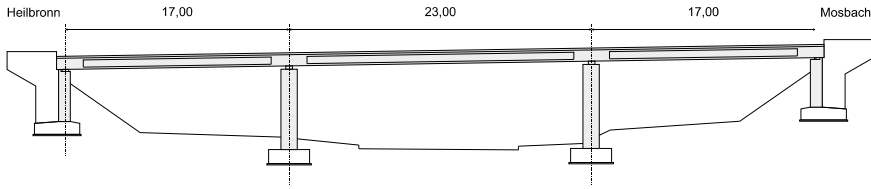


Fig. 2 Longitudinal view of the bridge (dimensions in meter)

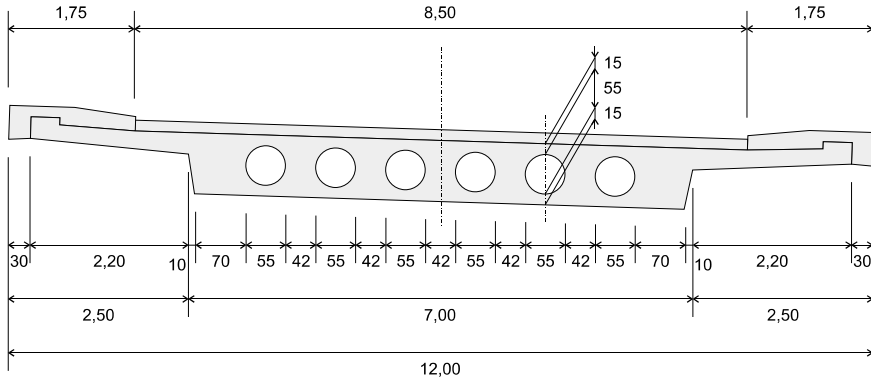


Fig. 3 Bridge's cross-section (dimensions in centimetre)

In addition to the high increase in traffic loads compared to the year of construction in 1964, and the corrosion-induced cracking risk, other critical problems may arise due to construction methods and the design standards adopted back then. Construction failures can already appear during construction caused by misplacement of the hollow-core bodies, and difficulties in compacting the surrounding concrete. From the structural point-of-view, the hollow-core bodies prevent two-axis load transfer and thus in the redistribution of forces in the transversal direction. Likewise, shear forces and temperature loads were not taken into account to the extent that it is considered necessary from today's standards at the time the building was planned. Finally, the hollow-core cannot be examined as part of the building inspection, which means that any damage inside them may not be early detected.

2.2 Monitoring System

A fibre-optic monitoring system based on long-gauge FBG (LGFBG) sensors were installed to continuously monitor strain and temperature changes, and vibration of the bridge superstructure.

The strain monitoring consists of two parallel measuring lines, each with 27 LGFBG sensors along the complete longitudinal direction, and five measuring lines

in the shear direction, with seven LGFBG sensors each. For every LGFBG strain sensor, an embedded temperature sensor is present for temperature compensation on the FO. Besides, the concrete temperature is monitored at five different points in the middle bridge field, and the acceleration is measured at 2 locations. The sensors were divided into eight quasi-distributed arrays equipped with redundancy connection fibres, which enable measurements to be continued if a primary connection cable fails. A schema of the sensors is given in Fig. 4 and overview photos are shown in Fig. 5. The following sensors are installed on the structure:

- Strain in the longitudinal direction - sensors S01-S54 and S80-89: For monitoring in the longitudinal direction, two distributed strain sensor-measuring lines are attached to the bottom of the bridge, located in the area of the prestressed cables. The sensors S80 to S89 were installed on the side of the structure at about 50 cm above the lower surface. The sensors S01 to S54 have a gauge length of 2.05 m, and the sensors S80 to S89 a gauge length of 0.50 m.
- Strain in the transverse direction – sensors S55-S79: Five strain sensor-measuring lines across the cross-section were installed on the underside of the bridge in the area of the maximum bending moments and on the two supports. These sensors have a gauge length of 1.35 m.
- Temperature sensors T01-T05: temperature sensors in the middle of the bridge, transverse to the direction of travel.

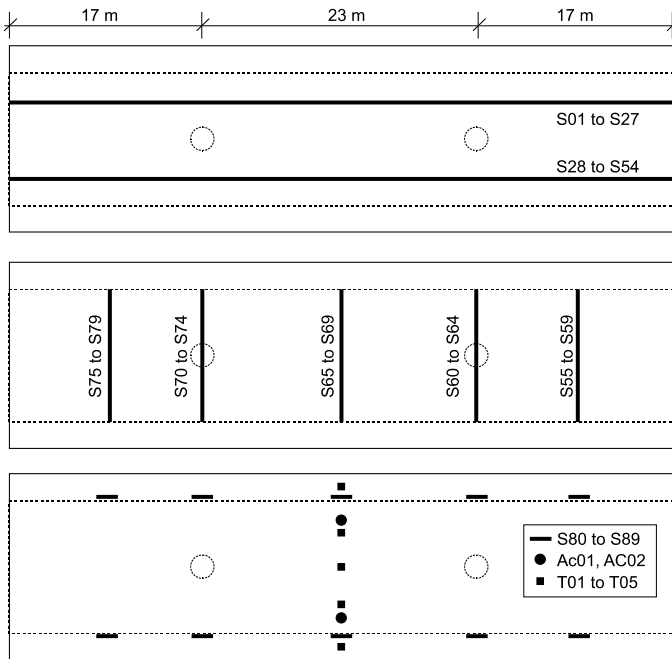


Fig. 4 Schema of the sensors' configuration (bottom view of the superstructure)



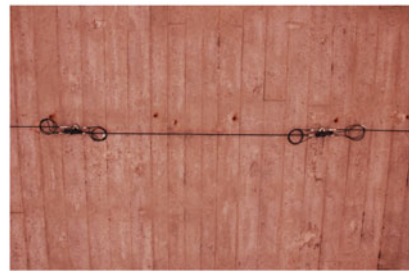
a. Overview of the bridge.



b. View of the configuration of the sensor



c. View of the configuration of the sensor



d. An LGFBG sensor with 2.05 m gauge.

Fig. 5 Overview of the bridge and the monitoring system

- Acceleration - sensors AC01-AC02: Two accelerometers with a vertical measuring direction in the middle of the main field each centred between the main axis and the edges of the support plate.

The optical interrogator was installed together with an industrial computer with an embedded LTE modem, a power bank supply to sustain power cuts up to 30 min, and additional components in a temperature-controlled control cabinet on the southern abutment. The measuring system can be entirely operated via remote access, which also enables the transfer of all stored files.

The measurement has been running continuously since 8th October 2019, with a measurement frequency of 200 Hz. All measurement data are available at any time for live visualisation. The data saving is only carried out if the measured change in strain is higher than a specified trigger. Also, a report is automatically generated every 15 min, in which the maximum, minimum and average values of all sensors are documented.

The monitoring system generates a considerable amount of data, given its high-frequency rate and the high sensor-count. To improve data management and the analysis of the results, the measured data is automatically stored in a MySQL database. The SQL database is accessed using customised MATLAB scripts written specifically for this application, where all the analysis and results, including graphics, are

automatically processed. After that, older measured data can be deleted to free up memory space.

3 First Measurement Data

The strain-variation measured by the longitudinal sensors during the crossing of a truck over the bridge is shown in Fig. 6. The graphics Fig. 6a–c represent the line of sensors at one side of the superstructure, while the graphic Fig. 6d–f the line of sensors on the opposite side (refer to). The vehicle was travelling in the direction from S01 to S27. The total duration of the measurement is 4 s, and it was acquired with a frequency of 200 Hz. Each curve presented in the graphics can be understood as

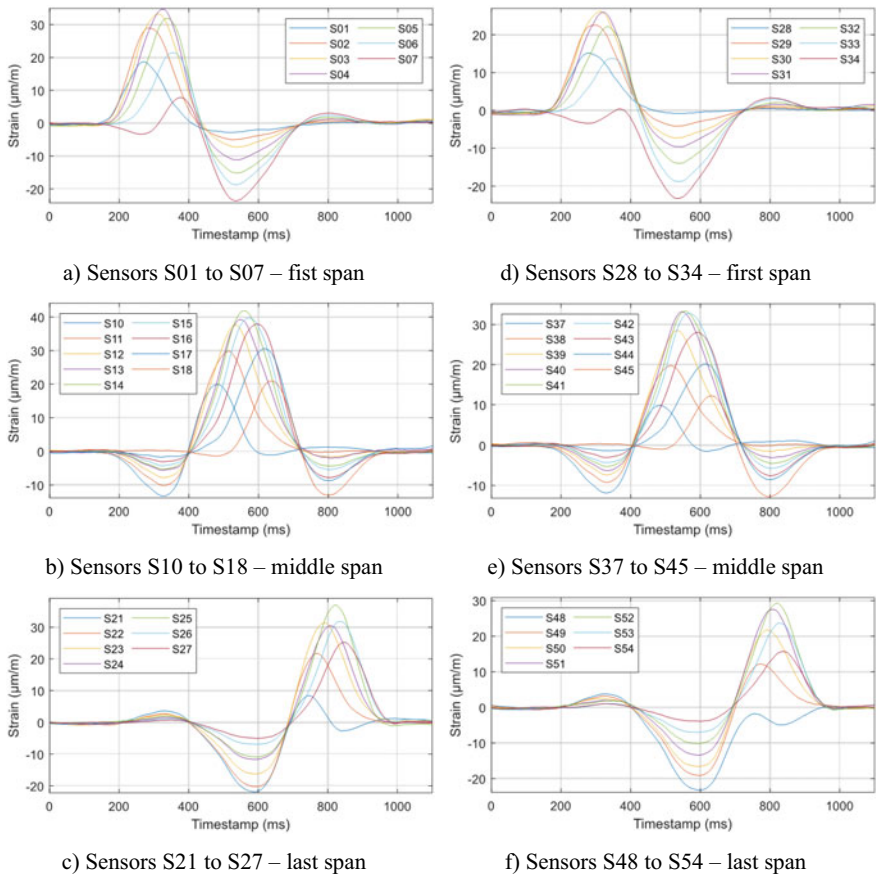


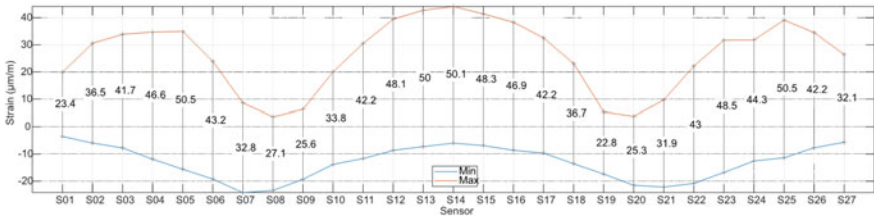
Fig. 6 Dynamic strain measurement of the LGFBG sensors located under the spans in the longitudinal direction during the crossing of a truck over the bridge

the strain influence line of the bridge sections corresponding to each of the installed sensors.

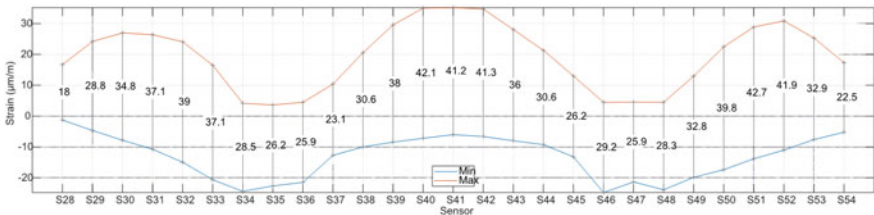
When the vehicle enters the bridge, the sensors S01 to S07 and S28 to S34, located under the first span, displayed peaks of positive strain, while the sensors S10 to S18 and S37 to S45, located in the middle span, measured negative strain, and, finally, all the sensors under the last span displayed values close to zero. When the vehicle passes over to middle span, it can be noted an inversion of the values' signal for all sensors, where now the sensors in the middle span display positive peaks and the sensors on both side-spans negative peaks.

The sensors also tend to converge to zero at the same timestamp when the vehicle passes above the two columns, around timestamps 400 and 700 ms, which is expected since the columns absorb the vehicle's load when it is standing over the column. At last, it is observed symmetric behaviour between the sensors in Fig. 6a–d on the first span and the sensors in Fig. 6c–f on the last span, as the vehicle crosses it and leaves the bridge superstructure.

In Fig. 7 is shown the maximum and minimum strain diagram for the longitudinal sensors. The two lines of LGFBG longitudinal sensors are represented separately in Fig. 7a for sensors S01 to S27, and in Fig. 7b for sensors S28 to S54. The amplitude, i.e. the difference between the maximum and the minimum strains, is plotted vertically for each sensor. Three positive strain peaks occur in the central region on each of the three spans, whereas the two negative peaks arise where the two centre columns are located. The maximum measured strain is 44.11 $\mu\text{m}/\text{m}$ on sensor S14, the minimum -24.36 $\mu\text{m}/\text{m}$ on sensors S34, and the maximum strain amplitude is 50.5 $\mu\text{m}/\text{m}$ on sensor S25.



a) Sensors S01 to S27



b) Sensors S28 to S54

Fig. 7 Maximum and minimum strain diagram for the longitudinal LGFBG sensors during the crossing of a truck over the bridge

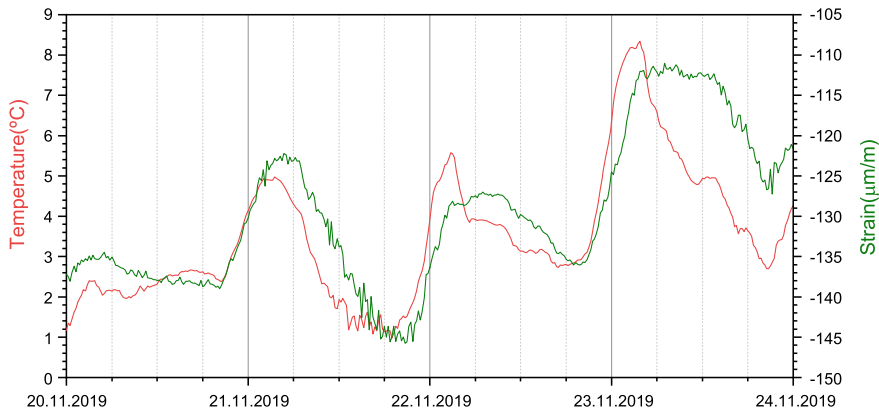
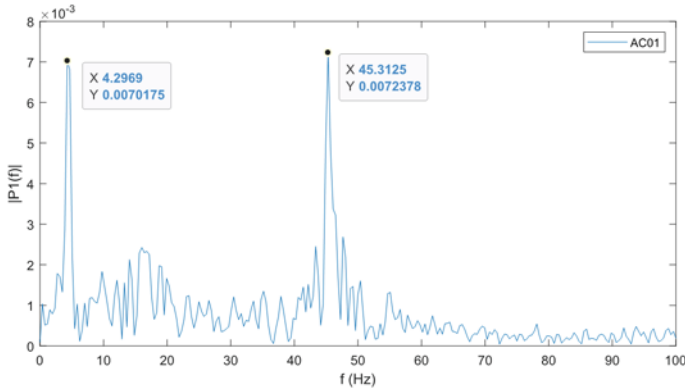


Fig. 8 Influence of the temperature variation on the measured strain during four days

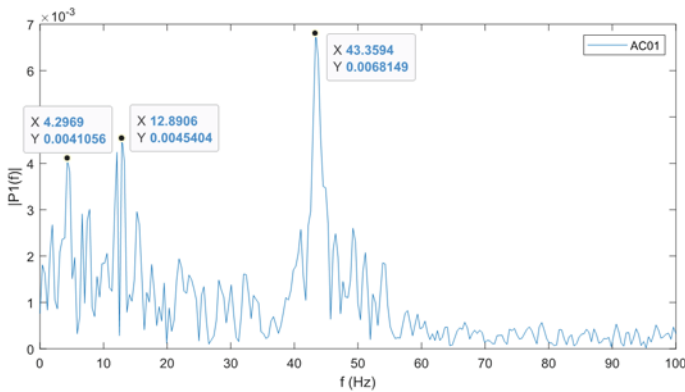
Figure 8 shows an example of the measured strains and temperatures on sensor S41 over four days. It can be seen that the strain variation follows the temperature curve. The phase shift and the damping of individual measurement peaks from solar radiation are a consequence of the temperature inertia of the reinforced concrete. So far, it has been found that the changes in elongation at all sensors due to the temperature fluctuations, with a maximum of $180 \mu\text{m/m}$ so far, are significantly bigger than the strains from traffic loads with a maximum of $40 \mu\text{m/m}$ so far. For each Celsius temperature increase, the bridge stretches approx. $8 \mu\text{m/m}$ in the longitudinal direction, meaning a coefficient of thermal expansion of $8 \times 10^{-6} \text{ }^\circ\text{C}^{-1}$, which is in the range of the literature value for concrete according to DIN 1045–1 (between 5 and $14 \times 10^{-6} \text{ }^\circ\text{C}^{-1}$).

Figure 9 shows the single-sided amplitude spectrums for the sensors AC01 on two different events where a large truck drove over the bridge. The FFT was done using 1024 samples taken from a measurement at 200 Hz and smoothed using a Hanning window. It can be seen two prominent peaks at 45.3 Hz in the first event and 43.4 Hz in the second event.

The authors believe that the reliability and precision of the measure data combined with the continuously high-frequency measurements will allow an in-depth analysis of the structure's actual condition and remaining lifetime. With algorithms such as the rain flow analysis it is possible to access the more repetitive, with smaller amplitude load cycles due to the traffic and the more spaced, with greater amplitude load cycles due to the temperature shift along the year. The comprehensive strain and temperature distribution in both the longitudinal and the transversal direction enable the calibration of numerical models to identify local degradation of the structure's stiffness, and thermos-energetic models to a better understanding of the temperature influence within the bridge.



a) Event on 8th January, 11:53h A.M.



b) Event on 20th January, 07:11h A.M.

Fig. 9 Single-Sided Amplitude Spectrum for sensor AC01 during the crossing of a truck over the bridge in two different instances

4 Conclusion

This work presented the deployment of a large-scale application of fibre optic-based sensors for structural health monitoring of a prestressed concrete bridge, and its initial results obtained during operation.

The use of long-gauge FBG sensors has the potential to delivery in-depth knowledge of the strain distribution and the structural behaviour of large civil infrastructures. The dynamic measurements allow the representation of the strain influence line in each section of the bridge covered by a sensor and can be used for the detection of local damages, such as crack openings and the rupture of prestressed cables, as well as the influence of temperature variation loads and the structure’s remaining lifetime.

Due to the continuous monitoring, the system can be set-up to notify extreme events, such as an abrupt shift of the strain measurement, increasing public safety.

The high resolution of the measurement data along with numerical analysis would allow an estimation of the actual traffic loads and damage state on the bridge after calibration.

Acknowledgements The authors would like to acknowledge the Brazilian Federal Agency for Support and Evaluation of Graduate Education (CAPES, finance code 001), the Federal University of the Jequitinhonha and Mucuri Valleys (UFVJM, Brazil), the Materials Testing Institute University of Stuttgart (MPA, Germany), and the Regional Council of Stuttgart (RPS, Germany), which collectively funded this work.

References

1. An, Y., Spencer, B.F., Ou, J.: A test method for damage diagnosis of suspension bridge suspender cables. *Computer Aided Civil Infrast. Eng.* **30**(10), 771–784 (2015). <https://doi.org/10.1111/mice.12144>
2. Cho, S., Giles, R.K., Spencer, B.F.: System identification of a historic swing truss bridge using a wireless sensor network employing orientation correction. *Struct. Control Health Monit.* **22**(2), 255–272 (2015). <https://doi.org/10.1002/stc.1672>
3. Giles, R.K., Spencer Jr, B.F.: Development of a long-term, multimetric structural health monitoring system for a historic steel truss swing bridge (2015)
4. Glisic, B., Inaudi, D.: Development of method for in-service crack detection based on distributed fiber optic sensors. *Struct. Health Monit.* **11**(2), 161–171 (2012). <https://doi.org/10.1177/1475921711414233>
5. Huang, J., Zhou, Z., Zhang, D., Yao, X., Li, L.: Online monitoring of wire breaks in prestressed concrete cylinder pipe utilising fibre Bragg grating sensors. *Measurement* **79**, 112–118 (2016). <https://doi.org/10.1016/j.measurement.2015.10.033>
6. Kudva, J.N., Marantidis, C., Gentry, J.D., Blazic, E.: Smart structures concepts for aircraft structural health monitoring. In: *SPIE Proceedings*. SPIE, pp. 964–971 (1993). <https://doi.org/10.1117/12.152828>
7. Lopez-Higuera, J.M., Cobo, L.R., Incera, A.Q., Cobo, A.: Fiber optic sensors in structural health monitoring. *J. Lightwave Technol.* **29**(4), 587–608 (2011). <https://doi.org/10.1109/JLT.2011.2106479>
8. Mahadevan, S., Adams, D., Kosson, D.: Challenges in concrete structures health monitoring. In: Daigle, M.J., Bregon, A. (eds.) *Annual Conference of the Prognostics and Health Management Society 2014*. Fort Worth, TX, USA, pp. 561–567 (2014)
9. Phares, B.M., Washer, G.A., Rolander, D.D., Graybeal, B.A., Moore, M.: Routine highway bridge inspection condition documentation accuracy and reliability. *J. Bridg. Eng.* **9**(4), 403–413 (2004). [https://doi.org/10.1061/\(ASCE\)1084-0702](https://doi.org/10.1061/(ASCE)1084-0702)
10. Sakiyama, F.I.H., Lehmann, F.A., Garrecht, H.: Structural health monitoring of concrete structures using fibre optic based sensors: a review. *Mag. Concr. Res.* 1–45, (2019). <https://doi.org/10.1680/jmacr.19.00185>
11. Udd, E., Spillman, W.B.: *Fiber optic sensors. An introduction for engineers and scientists* (2nd ed.). John Wiley & Sons, Hoboken N.J. (2011)

12. Wu, B., Wu, G., Yang, C., He, Y.: Damage identification and bearing capacity evaluation of bridges based on distributed long-gauge strain envelope line under moving vehicle loads. *J. Intell. Mater. Syst. Struct.* **27**(17), 2344–2358 (2016). <https://doi.org/10.1177/1045389X16629571>
13. Ye, X.W., Su, Y.H., Han, J.P.: Structural health monitoring of civil infrastructure using optical fiber sensing technology: a comprehensive review. *Scientif. World J.* **652329**, (2014). <https://doi.org/10.1155/2014/652329>